5. E. Mankinen and G. B. Dalrymple, *Earth Planet. Sci. Lett.* **17**, 89 (1972).
6. G. B. Dalrymple and M. A. Lanphere, *Potassium-Argon Dating: Principles, Techniques and Applications to Geochronology* (Freeman, San Francisco, 1969).
7. C. O. Ingamells, *Anal. Chim. Acta* **52**, 323 (1970).
8. E. O. Jackson, E. A. Silver, G. B. Dalrymple, *Geol. Soc. Am. Bull.* **83**, 601 (1972).
9. I. McDougall, *ibid.* **75**, 107 (1964).
10. A. R. McBirney and K. Aoki, in *The Galápagos*, R. I. Bowman, Ed. (Univ. of California Press, Berkeley, 1966).
11. A. V. Cox and G. B. Dalrymple, *Nature (London)* **209**, 776 (1966).
12. R. N. Anderson, D. A. Clague, K. D. Klitgord, M. Marshall, R. K. Nishimori, *Geol. Soc. Am. Bull.* **86**, 683 (1975).
13. E. M. Herron, *Geol. Soc. Am. Bull.* **83**, 1671 (1972).
14. F. J. Swanson, H. W. Baitis, J. Lexa, J. Dymond, *ibid.* **85**, 1803 (1974).
15. T. H. Van Andel, G. R. Heath, B. T. Malfait, D. F. Heinrichs, J. I. Ewing, *ibid.* **82**, 1489 (1971).
16. Potassium-argon dating was done at the U.S. Geological Survey, Menlo Park, under the direction of G. B. Dalrymple, who also reviewed the manuscript. A. L. Berry and S. J. Kover assisted with the argon and potassium measurements. J. R. Sulat provided computer programming. A. V. Cox collected most of the samples; his comments and field notes were helpful. Further samples and pertinent information came from G. B. Dalrymple, H. Williams, J. W. Durham, and K. A. Howard.

17 November 1975; revised 29 January 1976

Differing Attenuation Coefficients of Normal and Infarcted Myocardium

Abstract. *There are significant differences in attenuation coefficients between normal and infarcted myocardium measurable with a computerized transaxial tomographic scanner. Additionally, iodinated contrast material administered prior to killing the test animals resulted in excellent visualization of the blood-myocardial interface at a time when standard radiographs detected no differences between the ventricular cavity and the myocardial wall. These natural and induced changes in attenuation coefficients offer a new approach to evaluating and understanding the processes of tissue injury and death. Their clinical relevance lies in application to the twin problems of myocardial infarction and the structure and function of the cardiac wall.*

The accurate detection and sizing of infarcted myocardium is of major experimental and clinical importance. It represents an essential step in developing an in vivo approach to the study of tissue infarction and necrosis. In the clinical setting, it not only permits the diagnosis of acute infarction but also is vital in evaluating interventions designed to limit the degree to which ischemic heart muscle goes on to cellular death (*1*).

At present, the most useful approach to visualizing the volume of infarcted tissue employs radionuclides (*2*, *3*). This method is limited by both image resolution and heterogeneous tissue uptake of the isotope. Current methods of delineating the cardiac chambers generally employ invasive intracardiac catheterization and the rapid delivery of an iodinated contrast agent, recorded serially on cine or large film. Noninvasive methods, such as radionuclide imaging and echocardiography, have significant limitations of resolution and extent of visualization.

The delineation of normal and abnormal myocardium and visualization of the cardiac chambers could be readily accomplished by noninvasive means if there were detectable differences in x-ray absorption by normal myocardium, ischemic or dead myocardium, and the intracavitary blood pool. In this study we evaluated whether the differing tissue compositions were adequate to register altered images on computerized transaxial tomograms (CTT) and the degree to which physiologic doses of contrast agent might enhance visualization of the myocardial wall.

Five normal mongrel dogs weighing 14 to 20 kg were killed immediately after receiving, intravenously, 5000 units of aqueous heparin. In addition, one of these animals had received 1.0 ml/kg of a mixture of meglumine and sodium diatrozoate (37 percent iodine) (Renografin-76, E. R. Squibb & Sons, Princeton, N.J.) 5 minutes prior to death. Acute myocardial infarctions were created in four similar dogs by embolization of a radiopaque polyethylene plug into the left anterior descending coronary artery under fluoroscopic control (*2*). Two days later, 5000 units of aqueous heparin were administered intravenously and the animals were killed immediately. The hearts of all nine dogs were excised after ligation of the venae cavae, the hilar pulmonary arteries and veins, and the aorta. The excised hearts were shaken and placed in a divided plastic container (Tupperware Corp., Orlando, Fla.) which was filled with 0.9 percent sodium chloride and fitted snugly into the head cap of the EMI (EMI Medical Inc., Northbrook, Ill.) CTT scanner. The specimens were scanned at 120 or 140 kv; the scan thickness was either 8 or 13 mm. Attenuation coefficients were measured with the EMI scanner, which has a 160 by 160 matrix and has previously been described in detail (*4–7*).

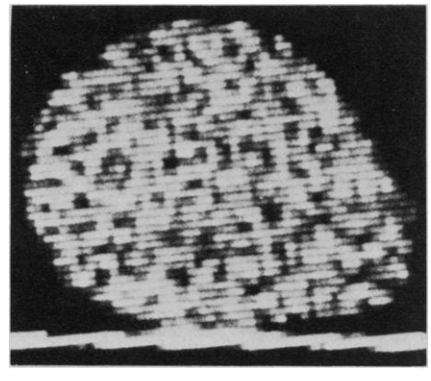

Fig. 1. Normal heart with no contrast agent given. Section at ventricular level showing uniform absorption with a value for myocardium of 26.0 ± 0.6 EMI units and for blood of 26.2 ± 1.0 EMI units.

Scans of representative areas of myocardial wall in normal hearts had uniform EMI values of 26.0 ± 0.6 EMI units (mean ± standard error of the mean). In these animals the intracavitary blood values were 26.2 ± 1.0 EMI units. [One EMI unit corresponds to approximately a 0.2 percent difference in x-ray attenuation coefficient compared to water (*7*)]. There was no consistent visualization of the myocardial-blood interface (Fig. 1). When the hearts were allowed to stand for a protracted interval, the red blood cells settled to the lower portion of the ventricular cavity, which became denser than the myocardial wall, while the plasma in the upper portion of the cavity was less dense.

The administration of contrast agent to the animals before they were killed resulted in a cavitary (blood pool) attenuation coefficient of 43 ± 1 EMI units, compared to a myocardial attenuation coefficient of 33 ± 1 EMI units, with consequent clear visualization of the blood–myocardial wall interface (Fig. 2). This difference of 10 EMI units corresponds to about 2 percent difference in the attenuation coefficients of intracavitary blood and myocardial wall. Despite the measurable difference in attenuation coefficient, high-quality, low-kilovoltage standard radiographs taken immediately after scanning failed to demonstrate any detectable difference in radiographic density between the myocardial wall and intracavitary blood.

The animals with myocardial infarctions showed three different scan patterns. In two animals the site of histologically confirmed infarction displayed attenuation coefficients 1 percent lower than in the surrounding normal myocardium (for example, infarct, 21.7 ± 1.2 EMI units compared to normal myocardium, 26.8 ± 1.0 EMI units) (Fig. 3a). In a third animal the attenuation coefficient

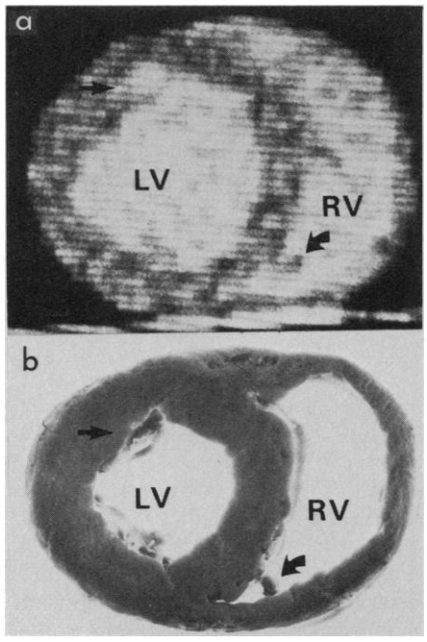

Fig. 2. (a) Computerized transaxial tomographic scan of normal heart at the level of the left ventricle (*LV*) and right ventricle (*RV*) after injection of 1 ml of Renografin-76 per kilogram 5 minutes before the animal was killed. Myocardial wall values, 33 ± 1 EMI units; ventricular cavity blood pool values, 43 ± 1 EMI units. (b) Slice of myocardial tissue taken at the same level. Note trabecular (arrows) detail on both scan and specimen.

of the infarcted tissue was 1 percent greater than that of the surrounding normal myocardium (infarct, 30.8 ± 1.7 EMI units; normal myocardium, 25.7 ± 1.4 EMI units) (Fig. 3b). By using multiple overlapping scans of known thickness, the localization and extent of infarction could be assessed in these animals. The fourth animal, whose histologic sections showed only a small subendocardial infarct, had no change (to within ± 0.2 percent) in attenuation coefficient in the affected area.

The infarctions with a reduced attenuation coefficient were grossly edematous, and the infarction with an increased attenuation coefficient was in the retraction stage of infarction with gross thinning of the wall readily apparent both on inspection of the specimen and on the CTT scan.

Since the original descriptions of computerized transaxial tomography (*4*, *5*), this technique has been widely applied to the study of intracranial abnormalities (*8*). Recently there has been considerable interest in applying CTT to the thorax and abdomen (*9*). We have demonstrated differences in attenuation coefficients between normal and infarcted myocardium which are most likely related to the known changes in intracellular ion concentrations and the size of the intercellular fluid compartment in infarcted hearts (*10*).

These measurable changes open up an entire new dimension for the sequential, in vivo evaluation of experimental models of ischemia and infarction. The spectrum of attenuation coefficient changes seen with acute infarctions, including lower values with edematous areas of infarction, higher values with thin retracted infarcts, and no detectable change when only a small subendocardial infarct is present, may provide a clinically useful approach to detecting and sizing transmural infarctions. The level and direction of change in attenuation coefficient probably relates to the different stages of infarction as seen on pathologic examination. This may prove helpful in dating acute infarctions. While the naturally occurring differences in attenuation coefficients of normal and infarcted muscle can be visualized, the utility of scanning may well be increased by enhancing these differences by prior intravenous administration of contrast material.

The difference between the attenuation coefficient of blood and myocardium seen after administration of the contrast agent in doses comparable to those used in man for intravenous urography indicates that computerized scanning may be a low-risk method of visualizing ventricular wall motion in vivo. Furthermore, the differences in attenuation coefficient between plasma and packed red cells suggest that the ventricular wall may be seen on CTT scans without contrast agent in patients with either very high or very low hematocrits.

On the basis of these data, an effective and reproducible method will require a CTT scanner capable of measuring and displaying differences in the attenuation coefficients of tissue of about 1 percent. A spatial resolution comparable to that of the EMI scanner (a few millimeters) is desirable. To achieve these characteristics, precise gating to the dynamic events of the heart cycle and acquisition of a series of images corresponding to different phases of that cycle may be required. These objectives are thought to be well within currently available technologic capabilities and should be pursued.

In the broadest view, such a scanner would be of considerable and immediate interest for its low-risk, noninvasive application to the following areas: (i) a new approach to experimental study of tissue ischemia, infarction, and necrosis; (ii) detection, sizing, and dating of acute myocardial infarctions and the evaluation of the effectiveness of mechanical and pharmacologic interventions designed to limit infarct size (*1*); (iii) evaluation of regional ventricular wall motion and thickness in acute and chronic myocardial ischemia; and (iv) overall assessment of ventricular function through measurement of ventricular volumes, ejection fractions, and other physiologic parameters.

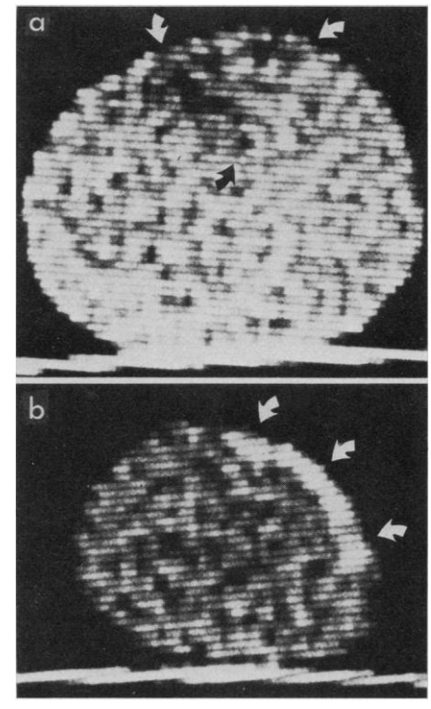

Fig. 3. (a) Computerized transaxial tomographic scan 2 days after infarction showing rim of tissue extending into the region of interventricular septum (arrows) with attenuation coefficients 5.1 EMI units less than the normal myocardium. This distribution of infarcted tissue was confirmed on the sectioned specimen. (b) Computerized transaxial tomographic scans 2 days after infarction showing a thinned rim of tissue with attenuation coefficients 5.1 EMI units higher than normal myocardium along the anterior left ventricular wall (arrows). This corresponded on the sectioned specimen to the region of infarction.

DOUGLASS F. ADAMS
SAMUEL J. HESSEL*
PHILIP F. JUDY, JAY A. STEIN
HERBERT L. ABRAMS
Department of Radiology, Harvard Medical School, and Peter Bent Brigham Hospital, Boston, Massachusetts 02115

References and Notes

1. E. Braunwald and P. R. Maroko, *Circulation* **50**, 206 (1974).
2. B. L. Holman, M. K. Dewanjee, J. Idoine, C. P. Fliegel, M. A. Davis, S. Treves, P. Eldh, *J. Nucl. Med.* **14**, 595 (1973).
3. F. J. Bonte, R. W. Parkey, K. D. Graham, J. Moore, E. M. Stokely, *Radiology* **110**, 473 (1974).
4. G. N. Hounsfield, *Br. J. Radiol.* **46**, 1016 (1973).
5. J. Ambrose *ibid.*, p. 1023.
6. P. F. J. New, W. R. Scott, J. A. Schnur, K. R. Davis, J. M. Taveras, *Radiology* **110**, 109 (1974).
7. E. C. McCullough, H. L. Baker, Jr., O. W.

Houser, D. F. Reese, *ibid.* **111**, 709 (1974).
8. J. Ambrose, *J. Neurosurg.* **40**, 679 (1974); D. Schellinger, G. Di Chiro, S. P. Axelbaum, H. L. Twigg, R. S. Ledley, *Radiology* **114**, 257 (1975); W. R. Scott, P. F. J. New, K. R. Davis, J. A. Schnur, *ibid.* **112**, 73 (1974).
9. R. L. Philips, and D. H. Stephens, *Radiology* **115**, 43 (1975); R. J. Alfidi, J. Haaga, T. F. Meaney, W. J. MacIntyre, L. Gonzalez, R. Tarar, M. D. Zelch, M. Boller, S. A. Cook, G. Jelden, *ibid.* **117**, 257 (1975); R. S. Pickering, R. R. Hattery, G. W. Hartman, K. E. Holley, *ibid.* **113**, 643 (1974).
10. J. T. Lie, P. C. Pairolero, K. E. Holley, J. T. McCall, H. K. Thompson, J. L. Titus, *Circulation* **51**, 860 (1975).
11. Supported in part by PHS grants GM18674, HL11668, and HL05832.
* James Picker Foundation Fellow in Academic Radiology.

30 January 1976

Antibodies to Histones and Histone-Histone Complexes: Immunochemical Evidence for Secondary Structure in Histone 1

Abstract. *Highly specific antibodies were raised to histone 1 (H1) and the histone complexes $H3_2$–$H4_2$ and H2A–H2B, isolated by salt extraction. Antibody to H1 could detect irreversible conformational changes in acid- or urea-treated H1. The antibodies showed different reactivities with chromosomes as compared to antibodies in acid-extracted histones and should be useful in studies of native chromatin and chromosome structure.*

Evidence for the existence of secondary structure in histones has been obtained from studies of circular dichroism, infrared and nuclear magnetic resonance (*1*), fluorescence anisotropy (*2*), and optical rotatory dispersion (*3*). The consensus is that histone fractions exist largely as random coils in solutions of low ionic strength. However, small increases in ionic strength or the addition of DNA gives rise to considerable helicity in all histones with the exception of histone 1 (H1), which is thought to assume an extended β-conformation (*4*). All these studies have been carried out with histones isolated from chromatin by acid extraction procedures, the assumption being that acid-induced conformational changes are largely reversible. Although acid-treated histones do assume α-helical conformation in salt solutions, there is no evidence that this is the same α-helical structure found in native histones. Moreover, evidence is growing (*5*, *6*) that the conformational changes of histones exposed to acids are irreversible. The question of whether histones revert to their respective native configurations after exposure to denaturing conditions must be answered if meaningful interpretations are to be derived from studies in vitro relating to nucleohistone function and structure and to histone-histone interactions (*7*).

Problems dealing with secondary structure are amenable to investigation by immunochemical methods (*8*). Although antibodies have been produced to calf thymus histone fractions (*9*–*11*), here, too, the histones used as antigens were isolated by procedures that included denaturing agents such as urea, guanidinium chloride, and dilute mineral acids. Inasmuch as the H1 monomer, the $H3_2$–$H4_2$ tetramer and the H2A–H2B oligomers can now be isolated by mild salt extraction procedures (*5*, *12*), we attempted to produce antibodies to such preparations and to determine whether they can be used to provide insight on the conformational characteristics of histones.

For the preparation of the histones, 30 g of frozen calf thymus was homogenized at 700 rev/min for 4 minutes (*13*) with the use of the grinding medium of Panyim *et al.* (*14*). Nuclei were washed once with grinding medium containing 0.5 percent (weight to volume) Triton X-100 and sedimented (SW 25.1 rotor) through a grinding medium that was 1.62*M* in sucrose (*15*). The pellets were washed again as above. Electron microscopy revealed mostly intact nuclei stripped of their outer nuclear membrane and attached ribosomes. Purified chromatin was obtained from two such preparations of nuclei by freeze-thawing and Dounce homogenization in hypotonic buffer containing ethylenediaminetetraacetate (EDTA) (*14*), followed by three washings with 0.25*M* NaCl–0.01*M* tris-HCl (*p*H 8.0). The H1 was extracted with 310 ml of 0.6*M* NaCl–0.05*M* sodium acetate buffer (*p*H 5.0), and the deoxyribonucleoprotein, from which most of the H1 had been removed, was sedimented by ultracentrifugation (36 hours at 2°C) in polycarbonate tubes (*16*). The deoxyribonucleoprotein was extracted further with 2.0*M* NaCl–0.05*M* sodium acetate (*p*H 5.0), sedimented and reextracted with 2.0*M* NaCl to give a mixture of $H3_2$–$H4_2$ tetramer and H2A–H2B oligomer. Histone solutions were desalted at 4°C by ultrafiltration through a UM10 membrane (Amicon) and lyophilized. About 1.4 g of total histone was recovered from 60 g of calf thymus, a yield that compared favorably with yields from direct extraction of washed calf thymus homogenates with acid (*17*). Histone 1 was purified by chromatography through a Sephadex G-100 column (2.5 by 95 cm) at 5°C; the other histones, present as complexes, were also purified (*12*). All solutions contained 0.05*M* $NaHSO_3$ as protease inhibitor (*18*).

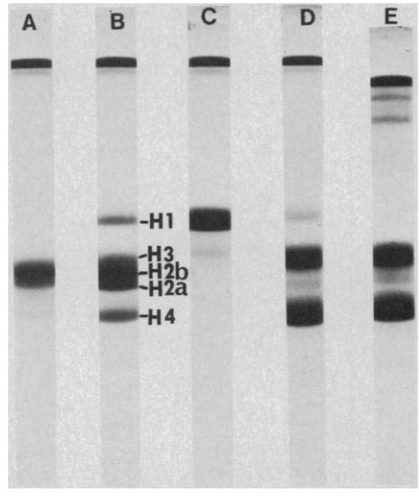

Fig. 1. Salt-extracted histones were subjected to electrophoresis for 3.5 hours in 15 percent acrylamide, 2.5*M* urea, 0.9*N* acetic acid, *p*H 2.7 (*24*). Histone 1 (25 μg) was added as a marker in each gel 1 hour before termination of electrophoresis (top band of each gel is the marker). Gel A, 25 μg of H2A–H2B; gel B, 50 μg of total histone; gel C, 50 μg of H1; gel D, 50 μg of $H3_2$–$H4_2$; gel E, 50 μg of $H3_2$–$H4_2$, from the second extraction with 2.0*M* NaCl. (Gel E was not processed at the same time as gels A, B, C, and D. The two extra bands immediately below the H1 marker in gel E represent degradation products of H1 resulting from storage at 4°C for 2 weeks. Freshly dissolved H1 was used as marker for gels A to D.) For immunization and complement fixation, histone antigens represented by gels A, C, and E were used. Histone complexes dissociate into their respective monomers under the electrophoretic conditions used.

Histone 1, $H3_2$–$H4_2$ tetramer [according to (*5*)], and H2A–H2B oligomer were pure as shown by polyacrylamide gel electrophoretic patterns (Fig. 1). For immunization, they were dissolved in saline (2 mg/ml) and emulsified with equal volumes of Freund's complete adjuvant (Difco) before each immunization. New Zealand white rabbits were injected with 0.1 ml every 7 days in each of four toepads. The 7*S* globulins were routinely obtained from all serums by fractionation on DEAE-cellulose (*19*); neutral 7*S* globulins were tested by a quantitative micro complement fixation technique in a total volume of 1.4 ml (*9*).

Specific antibodies were produced to H1, to the $H3_2$–$H4_2$ tetramer, and to the H2A–H2B oligomer. Antibodies to H1 had the highest serum titer at 80 percent complement fixation (1 : 9870, based on